Available online at www.sciencedirect.com
SCIENCE DIRECT®
Journal of Sound and Vibration 288 (2005) 177–193
JOURNAL OF SOUND AND VIBRATION
www.elsevier.com/locate/jsvi

Effect of material coupling on wave vibration of composite Euler–Bernoulli beam structures

C. Mei*

Department of Mechanical Engineering, The University of Michigan—Dearborn, 4901 Evergreen Road, Dearborn, MI 48128, USA

Received 3 May 2004; received in revised form 18 November 2004; accepted 30 December 2004
Available online 8 March 2005

Abstract

Fiber-reinforced composite materials are an important development in the continuing search for lightweight materials for great strength and stiffness. Lighter structures are usually more prone to vibrations. Furthermore, due to material coupling, composite beams normally vibrate with coupled vibration modes, which complicates vibration analysis. This paper presents the effect of coupling between bending and torsional deformations on vibrations of composite Euler–Bernoulli beams from a wave vibration standpoint. In the study, it is found that the torsional mode is only unaffected by the material coupling at low frequencies. The flexural modes are found affected over the entire frequency band. Unlike their uncoupled metallic counterparts, the wavenumbers for propagating and decaying wave components are no longer the same due to material coupling. Free vibration analysis is performed from a wave standpoint. Free vibration of composite beam with the coupling effect taken into account is of great importance. This is because the free vibration characteristics can be designed favorably by suitable choice of ply orientations and stacking sequence—one of the unique features of composite structures. Numerical examples for which comparative results are available in the literature are presented.

*Tel.: +1 313 593 5369; fax: +1 313 593 3851.
E-mail address: cmei@umich.edu.

0022-460X/$ - see front matter © 2005 Elsevier Ltd. All rights reserved.
doi:10.1016/j.jsv.2004.12.022

1. Introduction

Recent development of composite fibrous material has stimulated continuing research interests in exploring the possibility of constructing lightweight structures. When structures are made lighter, an accompanying side effect is that they are more prone to vibrations. Furthermore, as early as 1928, it was recognized that crystalline materials displayed anisotropic behavior with respect to arbitrarily oriented axes. Because of this anisotropy, the application of either a bending or twisting moment by itself produces both bending and twisting of a material specimen. Consequently, free vibration characteristics of slender composite beams with torsional and flexural material coupling are studied by investigators in the past few decades. Bending–torsion materially coupled composite beams of both solid and thin-walled cross-sections have been characterized in the literature by three cross-sectional stiffness parameters defined along a spanwise midsurface reference axis. The reference axis is chosen so that, the anisotropic composite beam would correspond to the elastic axis of a similar orthotropic structure without bend/torsion cross coupling [1]. These cross-sectional stiffness parameters are bending rigidity EI, torsional rigidity GJ and bending torsion material coupling rigidity K. The rigidity parameters can be found both theoretically and experimentally [1–3].

Taking into account of the coupling effect, a number of investigators have studied free vibrations of slender composite beam structures using various approaches, such as standard eigenvalue solution [2,4], exact numerical integration method, mixed finite element method and dynamic stiffness matrix approach [5–7]. In this paper, the effect of coupling on wave dispersion and vibrational modes of composite slender beam is investigated from a wave standpoint. The wave train closure principle [8] is applied in finding the natural frequencies of beam structures, which states that a natural frequency occurs if a wave component, after reflection at all boundaries along its path, returns to its starting point with the same amplitude and phase.

This paper is organized as follows. In the next section, the equation of motion for coupled bending torsion vibrations of an Euler–Bernoulli beam is presented and expressions for wavenumbers of the coupled systems derived. In Section 3, wave propagation and reflection characteristics of a clamped free beam are studied. In Section 4, free vibration analysis is performed, the wave train closure principle as well as conventional approach of letting equation of motion satisfy boundary conditions is applied in obtaining natural frequencies and mode shapes of the structure. In the application of wave train closure principle, the contributions to the dynamic responses from all possible wave components are taken into account. Hence the natural frequencies obtained are exact. The approach is illustrated through numerical examples for which comparative results are available in the literature. Concluding remarks are given in Section 5.

2. Equation of motion and dispersion characteristics

Fig. 1 shows a uniform composite beam with an unbalanced lay-up. Bending-torsion coupling is well known to occur for such configurations, as discussed earlier. The governing partial differential equations of motion for the coupled bending–torsional free vibration of a slender composite beam under the assumption that warping effect is negligibly small is

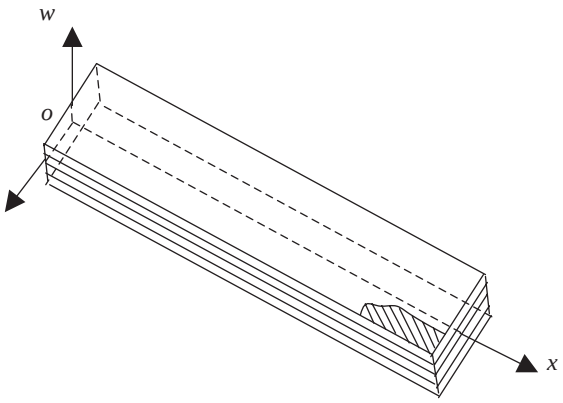

Fig. 1. Uniform composite beam with unbalanced lay-up.

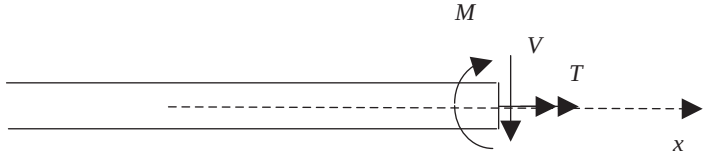

Fig. 2. Definition of positive shear force, torque and bending moment.

given by [4,7]

$$EI\,\frac{\partial^4 w(x,t)}{\partial x^4} + K\,\frac{\partial^3 \psi(x,t)}{\partial x^3} + \rho A\,\frac{\partial^2 w(x,t)}{\partial t^2} = 0, \tag{1a}$$

$$GJ\,\frac{\partial^2 \psi(x,t)}{\partial x^2} + K\,\frac{\partial^3 w(x,t)}{\partial x^3} - I_\alpha \frac{\partial^2 \psi(x,t)}{\partial t^2} = 0, \tag{1b}$$

where x is the position along the beam axis, t the time, $w(x,t)$ the transverse deflection of the center line of the beam, $\psi(x,t)$ the torsional rotation, I the area moment of inertia of cross section, I_α the polar mass moment of inertia per unit length about the x-axis, J the polar moment of inertia of the area of the cross-section, A is the cross-sectional area, and E, G and ρ are the Young's modulus, shear modulus and mass density, respectively.

It can be seen that Eqs. (1a) and (1b) are coupled through the torsional rotation and the transverse deflection of the structure.

Following the sign conventions of Fig. 2, the shear force $V(x,t)$, the bending moment $M(x,t)$ and the torque $T(x,t)$ at any section of the beam are related to the transverse deflection $w(x,t)$ and the torsional rotation $\psi(x,t)$ by

$$V(x,t) = EI\,\frac{\partial^3 w(x,t)}{\partial x^3} + K\,\frac{\partial^2 \psi(x,t)}{\partial x^2}, \tag{2}$$

$$M(x,t) = -EI\,\frac{\partial^2 w(x,t)}{\partial x^2} - K\,\frac{\partial \psi(x,t)}{\partial x}, \tag{3}$$

$$T(x,t) = K\,\frac{\partial^2 w(x,t)}{\partial x^2} + GJ\,\frac{\partial \psi(x,t)}{\partial x}. \tag{4}$$

Assuming time harmonic motion and using separation of variables, the solutions to Eqs. (1) can be written in the form $w(x,t) = w_0 e^{-ikx} e^{i\omega t}$ and $\psi(x,t) = \psi_0 e^{-ikx} e^{i\omega t}$, where i is the imaginary unit, ω the frequency, k the wavenumber, w_0 and ψ_0 the magnitudes of flexural deflection and torsional rotation respectively. Substituting the expressions for $w(x,t)$ and $\psi(x,t)$ into Eqs. (1) and rewriting the equations in matrix form, one has

$$\begin{bmatrix} EIk^4 - \rho A\omega^2 & iKk^3 \\ iKk^3 & -GJk^2 + I_\alpha \omega^2 \end{bmatrix} \begin{bmatrix} w_0 \\ \psi_0 \end{bmatrix} = 0. \tag{5}$$

Setting the determinant of matrix

$$\begin{bmatrix} EIk^4 - \rho A\omega^2 & iKk^3 \\ iKk^3 & -GJk^2 + I_\alpha \omega^2 \end{bmatrix}$$

to zero gives a third-order polynomial in k^2—the dispersion equation:

$$(EIk^4 - \rho A\omega^2)(-GJk^2 + I_\alpha \omega^2) + K^2 k^6 = 0. \tag{6}$$

Noting that when setting the coupling coefficient K to zero, one obtains the well-known wavenumbers of the uncoupled positive and negative going bending propagating, bending decaying and torsional propagating waves $e^{\mp ik_b x}$, $e^{\mp k_b x}$ and $e^{\mp ik_t x}$ as

$$k_b = \sqrt[4]{\frac{\rho A\omega^2}{EI}} \quad \text{and} \quad k_t = \sqrt{\frac{I_\alpha}{GJ}}\,\omega. \tag{7}$$

It can be seen from Eq. (7) that the uncoupled waves are dispersive, in that the phase velocity ω/k is frequency dependent.

In terms of the uncoupled wavenumbers, the coupled dispersion equations can be rewritten as

$$-\frac{K^2}{EIGJ}\,k^6 + (k^4 - k_b^4)(k^2 - k_t^2) = 0. \tag{8}$$

Expanding Eq. (8) gives

$$\left(1 - \frac{K^2}{EIGJ}\right)k^6 - k_t^2 k^4 - k_b^4 k^2 + k_t^2 k_b^4 = 0. \tag{9}$$

The explicit solutions to the above third-order polynomial in terms of k^2 can be found in most mathematical handbooks. This paper is not concerned with detailed study of the roots, therefore no elaboration is necessary. The focus is on the effect of coupling on the flexural and bending vibrations.

Both strain energy consideration and stiffness matrix condition require that [1,9]

$$\frac{K^2}{EIGJ} < 1 \quad \text{or} \quad -1 < \frac{K}{\sqrt{EIGJ}} < 1. \tag{10}$$

For the convenience of discussion, let us rewrite Eq. (9), the cubic equation in terms of k^2, in the form of

$$ax^3 + bx^2 + cx + d = 0, \tag{11}$$

where

$$x = k^2, \quad a = 1 - \frac{K^2}{EIGJ}, \quad b = -k_t^2, \quad c = -k_b^4 \quad \text{and} \quad d = k_t^2 k_b^4. \tag{12}$$

From Eqs. (7), (10)–(12), it is known that

$$a > 0, \quad b < 0, \quad c < 0 \quad \text{and} \quad d > 0. \tag{13}$$

It has been proved that the roots of Eq. (11), x_1 x_2 and x_3, are all real [7]. Furthermore, the roots are related to coefficients a, b, c and d by [10]

$$x_1 + x_2 + x_3 = -\frac{b}{a}, \quad x_1 x_2 x_3 = -\frac{d}{a}, \quad \frac{1}{x_1} + \frac{1}{x_2} + \frac{1}{x_3} = -\frac{c}{d}. \tag{14a–c}$$

Eqs. (13) and (14b) require that the three real roots x_1, x_2 and x_3 to be either all negative or one negative and two positive. Eqs. (13) and (14a) do not allow the three roots to be all negative. As a result, the signs of the three real roots to the cubic equation in terms of k^2 are two positives and one negative, which correspond to two propagating waves and one decaying wave respectively. From the above analysis, one can conclude that the material coupling does not affect the types of wave components in the structure; that is, there still exists two propagating waves and one decaying wave: flexural propagating wave, torsional propagating wave, and flexural decaying wave. Which is the same as materially uncoupled beams subjected to torsion and bending. However, the values of wavenumbers are affected by the coupling, as is not difficult to see from the coupled dispersion Eq. (8).

To examine the effect of material coupling on wave dispersion, two numerical examples are studied. The physical parameters of the composite beam are as listed in Table 1. For the purpose of comparison, the parameters are chosen from available literature. The first set of data was used by Refs. [2,6,7]. The beam is a thin 12-ply strip of carbon-fiber-reinforced plastic material with $\lfloor 45^\circ/0^\circ \rfloor_{3s}$ lay-up. The second set of parameters was used by Refs. [2,4,7]. It is a flat rectangular

Table 1
Physical parameters of example composite beams

Parameters	Bending rigidity EI (Nm^2)	Torsional rigidity GJ (Nm^2)	Coupling rigidity K (Nm^2)	Polar mass moment of inertia (kgm)	Density ρ (mg/m^3)	Width b (m)	Depth h (m)	Length L (m)
Beam 1	0.5317	0.3586	0.0990	1.66×10^{-6}	4557	0.03	0.00054	0.56
Beam 2	0.0143	0.0195	0.00632	5.562×10^{-6}	1469	0.03	0.00054	0.56

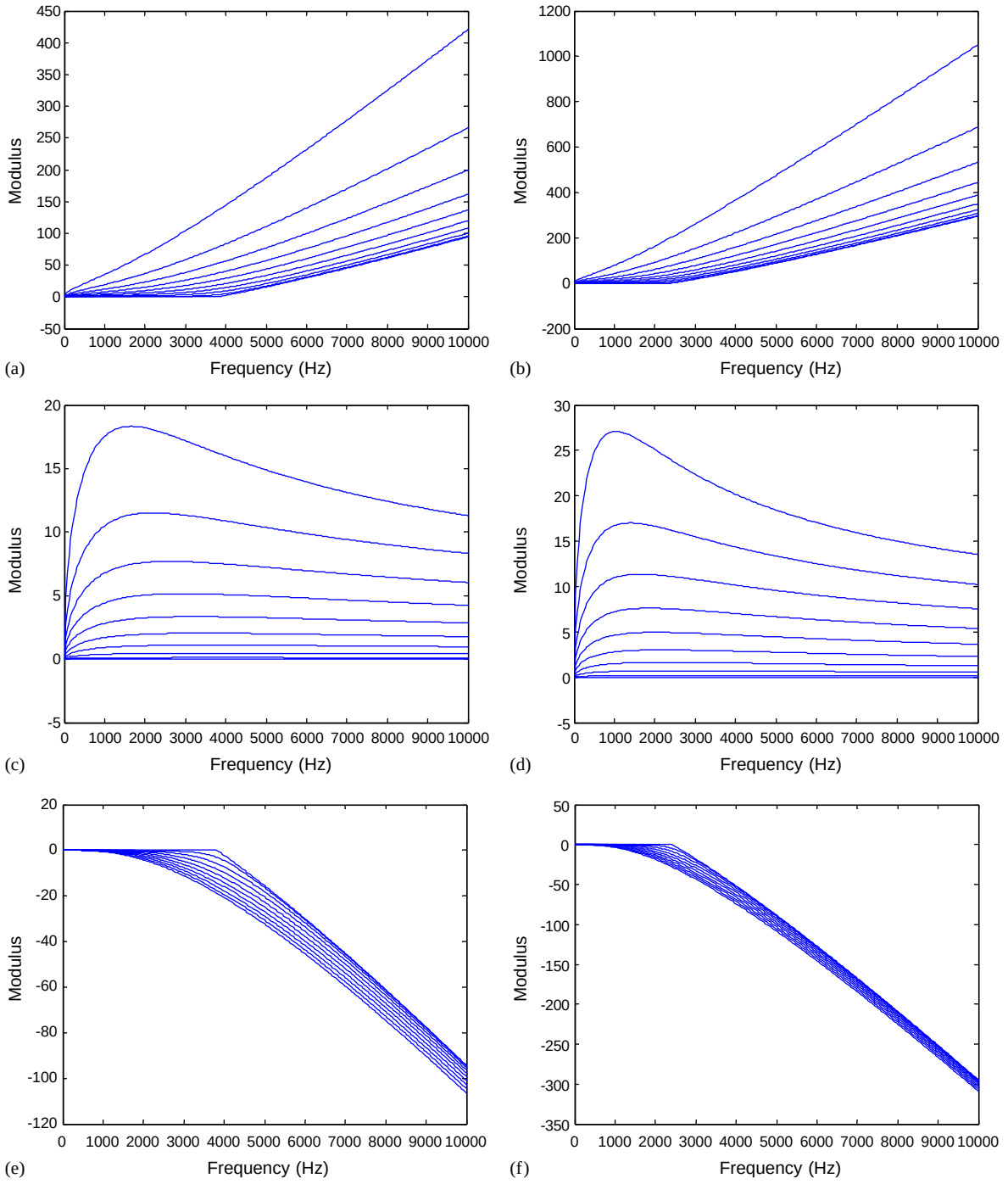

Fig. 3. Difference in wavenumber with and without coupling of (a) bending propagating waves in beam 1, (b) bending propagating waves in beam 2, (c) bending decaying waves in beam 1, (d) bending decaying waves in beam 2, (e) torsional propagating waves in beam 1, (f) torsional propagating waves in beam 2.

cross-section carbon-epoxy composite beam with stacking sequence $\lfloor 45^\circ/0^\circ \rfloor_s$. From the length-to-width and length-to-depth ratios, it can be seen that both beams can be considered as slender beams [11].

Fig. 3 shows the difference in wavenumber dispersion characteristics of torsional and flexural vibrations of the example composite beams with and without material coupling. From which it can be seen that the dispersion characteristics of the torsional wave at low frequencies are not affected by the material coupling. The dispersion characteristics of the flexural waves, however, are found altered by the material coupling over the entire frequency band. Consequently, the material coupling in general modifies both natural frequencies and mode shapes of the structure.

Under the situation when only lower frequency modes are of interest, due to the fact that at these frequencies the dispersion characteristics of the torsional wave remain almost identical with and without material coupling, the flexural wavenumbers of the propagating wave component k_{b1} and the decaying wave component k_{b2} of the coupled system are related to the uncoupled wavenumbers k_b and k_t as

$$k_{b1} = \frac{A + \sqrt{A^2 - 4B}}{2} \quad \text{and} \quad k_{b2} = \frac{A - \sqrt{A^2 - 4B}}{2}, \tag{15}$$

where

$$A = \frac{1-a}{a} k_t^2 \quad \text{and} \quad B = -\frac{k_b^4}{a}. \tag{15a}$$

With the time dependence $e^{i\omega t}$ suppressed, the solutions to Eqs. (1) are written as

$$\psi(x) = a_1^+ e^{-ik_1 x} + a_2^+ e^{-ik_2 x} + a_3^+ e^{-k_3 x} + a_1^- e^{ik_1 x} + a_2^- e^{ik_2 x} + a_3^- e^{k_3 x}, \tag{16}$$

$$w(x) = \overline{a_1^+} e^{-ik_1 x} + \overline{a_2^+} e^{-ik_2 x} + \overline{a_3^+} e^{-k_3 x} + \overline{a_1^-} e^{ik_1 x} + \overline{a_2^-} e^{ik_2 x} + \overline{a_3^-} e^{k_3 x}, \tag{17}$$

where k_1, k_2 and k_3 are wavenumbers of the torsional propagating, bending propagating and bending decaying components respectively. The wavenumbers can be solved from Eq. (9) or, at lower frequencies, approximated using k_t, k_{b1} and k_{b2} as discussed above.

Clearly the wave amplitudes a of $\psi(x)$ and $\bar{a}$ of $w(x)$ are related to each other. The relation can be found from Eq. (5) as

$$\frac{\overline{a_1^+}}{a_1^+} = -iP_1, \quad \frac{\overline{a_2^+}}{a_2^+} = -iP_2, \quad \frac{\overline{a_3^+}}{a_3^+} = -P_3, \quad \frac{\overline{a_1^-}}{a_1^-} = iP_1, \quad \frac{\overline{a_2^-}}{a_2^-} = iP_2, \quad \frac{\overline{a_3^-}}{a_3^-} = P_3, \tag{18}$$

where

$$P_1 = \frac{K}{EI}\left(\frac{k_1^3}{k_1^4 - k_b^4}\right), \quad P_2 = \frac{K}{EI}\left(\frac{k_2^3}{k_2^4 - k_b^4}\right) \quad \text{and} \quad P_3 = -\frac{K}{EI}\left(\frac{k_3^3}{k_3^4 - k_b^4}\right). \tag{18a}$$

3. Wave propagation and reflection

From a wave vibration standpoint, vibrations that propagate along a beam component are reflected and transmitted by discontinuities and boundaries. The propagation is governed by the

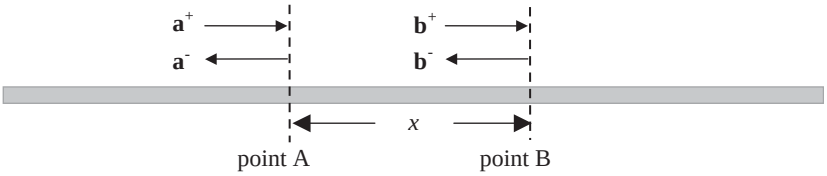

Fig. 4. Wave propagation.

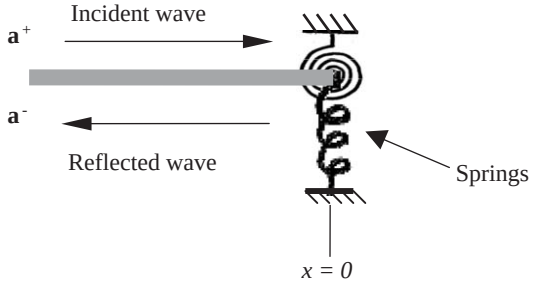

Fig. 5. Wave reflection at a general boundary.

so-called propagation matrix, and the reflection and transmission by the reflection and transmission matrices.

3.1. Propagation matrix

Consider two points A and B on a torsionally and flexually vibrating uniform beam a distance x apart, as shown in Fig. 4. Waves propagate from one point to the other, with the propagation being determined by the appropriate wavenumber. Denoting the positive and negative going wave vectors at points A and B as $\mathbf{a}^+$ and $\mathbf{a}^-$, and $\mathbf{b}^+$ and $\mathbf{b}^-$ respectively, they are related by

$$\mathbf{a}^- = \mathbf{f}(x)\mathbf{b}^-, \quad \mathbf{b}^+ = \mathbf{f}(x)\mathbf{a}^+, \tag{19}$$

where

$$\mathbf{f}(x) = \begin{bmatrix} e^{-ik_1 x} & 0 & 0 \\ 0 & e^{-ik_2 x} & 0 \\ 0 & 0 & e^{-k_3 x} \end{bmatrix} \tag{19a}$$

is known as the propagation matrix for a distance x.

3.2. Reflection matrices at boundaries

A general boundary condition is shown in Fig. 5. The incident waves $\mathbf{a}^+$ give rise to reflected waves $\mathbf{a}^-$, which are related by

$$\mathbf{a}^- = \mathbf{r}\mathbf{a}^+. \tag{20}$$

The reflection matrix **r** can be determined by considering the boundary conditions, considering clamped and free boundaries as examples:

At a free end, one has

$$M = 0, \quad Q = 0, \quad T = 0. \tag{21}$$

At a clamped end, one has

$$\psi = 0, \quad w = 0, \quad \frac{\partial w}{\partial x} = 0. \tag{22}$$

From Eqs. (2)–(4), (16)–(18), (22) and (20), the reflection matrix at the clamped end is found to be

$$\mathbf{r}_c = \begin{bmatrix} 1 & 1 & 1 \\ \mathrm{i}P_1 & \mathrm{i}P_2 & P_3 \\ P_1k_1 & P_2k_2 & -P_3k_3 \end{bmatrix}^{-1} \begin{bmatrix} -1 & -1 & -1 \\ \mathrm{i}P_1 & \mathrm{i}P_2 & P_3 \\ -P_1k_1 & -P_2k_2 & P_3k_3 \end{bmatrix}. \tag{23}$$

From Eqs. (16)–(18), (21) and (20), the reflection matrix at the free end is found as

$$\mathbf{r}_f = \begin{bmatrix} \frac{K}{EI}\mathrm{i}k_1 - \mathrm{i}P_1k_1^2 & \frac{K}{EI}\mathrm{i}k_2 - \mathrm{i}P_2k_2^2 & \frac{K}{EI}k_3 + P_3k_3^2 \\ -\frac{K}{EI}k_1^2 + P_1k_1^3 & -\frac{K}{EI}k_2^2 + P_2k_2^3 & \frac{K}{EI}k_3^2 + P_3k_3^3 \\ -\frac{K}{GJ}\mathrm{i}P_1k_1^2 + \mathrm{i}k_1 & -\frac{K}{GJ}\mathrm{i}P_2k_2^2 + \mathrm{i}k_2 & \frac{K}{GJ}P_3k_3^2 + k_3 \end{bmatrix}^{-1} \times \begin{bmatrix} \frac{K}{EI}\mathrm{i}k_1 - \mathrm{i}P_1k_1^2 & \frac{K}{EI}\mathrm{i}k_2 - \mathrm{i}P_2k_2^2 & \frac{K}{EI}k_3 + P_3k_3^2 \\ \frac{K}{EI}k_1^2 - P_1k_1^3 & \frac{K}{EI}k_2^2 - P_2k_2^3 & -\frac{K}{EI}k_3^2 - P_3k_3^3 \\ -\frac{K}{GJ}\mathrm{i}P_1k_1^2 + \mathrm{i}k_1 & -\frac{K}{GJ}\mathrm{i}P_2k_2^2 + \mathrm{i}k_2 & \frac{K}{GJ}P_3k_3^2 + k_3 \end{bmatrix}. \tag{24}$$

4. Free vibration analysis

4.1. Natural frequencies

4.1.1. Applying the wave-train closure principle

The propagating and reflection matrices can be combined for free vibration analysis of bending–torsion coupled composite beams.

Fig. 6 shows a general beam structure with boundaries A and B. Now consider the free response of this structure. Denoting the incident and reflected waves at boundaries A and B as $\mathbf{a}^-$,$\mathbf{a}^+$ $\mathbf{b}^+$ and $\mathbf{b}^-$ respectively, the relationships between the different waves are given as

$$\mathbf{a}^+ = \mathbf{r}_A\mathbf{a}^-, \quad \mathbf{b}^- = \mathbf{r}_B\mathbf{b}^+, \quad \mathbf{a}^- = \mathbf{f}(L)\mathbf{b}^-, \quad \mathbf{b}^+ = \mathbf{f}(L)\mathbf{a}^+, \tag{25}$$

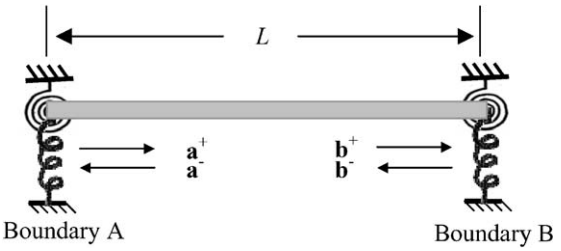

Fig. 6. A uniform beam structure with boundaries A and B.

where $\mathbf{r}_A$ and $\mathbf{r}_B$ are the reflection matrices at boundaries A and B respectively and $\mathbf{f}(L)$ is the propagation matrix between A and B that is L distance apart.

Solving Eqs. (25) gives

$$[\mathbf{r}_A\mathbf{f}(L)\mathbf{r}_B\mathbf{f}(L) - \mathbf{I}]\mathbf{a}^+ = \mathbf{0}, \tag{26}$$

where $\mathbf{I}$ denotes the identity matrix. For a non-trivial solution, it follows that

$$|\mathbf{r}_A\mathbf{f}(L)\mathbf{r}_B\mathbf{f}(L) - \mathbf{I}| = \mathbf{0}. \tag{27}$$

Eq. (27) is the characteristic equation from which the natural frequencies of the composite beam can be found. In the case of a clamped free beam, one has

$$|\mathbf{r}_c\mathbf{f}(L)\mathbf{r}_f\mathbf{f}(L) - \mathbf{I}| = \mathbf{0}. \tag{28}$$

4.1.2. Letting the equation of motion satisfy boundary conditions

The principle of this approach, that is allowing the equation of motion satisfying boundary conditions, represents the conventional concept of free vibration analysis. From a wave standpoint, the approach is described using the same example cantilevered uniform composite beam of length L, for which one has

$$\psi(x) = a_1^+ e^{-ik_1x} + a_2^+ e^{-ik_2x} + a_3^+ e^{-k_3x} + a_1^- e^{ik_1(x-L)} + a_2^- e^{ik_2(x-L)} + a_3^- e^{k_3(x-L)}, \tag{29}$$

$$w(x) = -iP_1a_1^+ e^{-ik_1x} - iP_2a_2^+ e^{-ik_2x} - P_3a_3^+ e^{-k_3x} + iP_1a_1^- e^{ik_1(x-L)} + iP_2a_2^- e^{ik_2(x-L)} + P_3a_3^- e^{k_3(x-L)}. \tag{30}$$

To satisfy the clamped boundary conditions given by Eq. (22), with origin chosen at the clamped end, one has

$$\begin{gathered} a_1^+ + a_2^+ + a_3^+ + a_1^- e^{-ik_1L} + a_2^- e^{-ik_2L} + a_3^- e^{-k_3L} = 0, \\ -iP_1a_1^+ - iP_2a_2^+ - P_3a_3^+ + iP_1a_1^- e^{-ik_1L} + iP_2a_2^- e^{-ik_2L} + P_3a_3^- e^{-k_3L} = 0, \\ -P_1k_1a_1^+ - P_2k_2a_2^+ + P_3k_3a_3^+ - P_1k_1a_1^- e^{-ik_1L} - P_2k_2a_2^- e^{-ik_2L} + P_3k_3a_3^- e^{-k_3L} = 0. \end{gathered} \tag{31}$$

To satisfy the free boundary conditions given by Eq. (21), one has

$$\begin{aligned}
&\left(-\frac{K}{EI}\,\mathrm{i}k_1+\mathrm{i}P_1k_1^2\right)a_1^+\mathrm{e}^{-\mathrm{i}k_1L}+\left(-\frac{K}{EI}\,\mathrm{i}k_2+\mathrm{i}P_2k_2^2\right)a_2^+\mathrm{e}^{-\mathrm{i}k_2L}+\left(-\frac{K}{EI}\,k_3-P_3k_3^2\right)a_3^+\mathrm{e}^{-k_3L}\\
&\quad-\left(-\frac{K}{EI}\,\mathrm{i}k_1+\mathrm{i}P_1k_1^2\right)a_1^--\left(-\frac{K}{EI}\,\mathrm{i}k_2+\mathrm{i}P_2k_2^2\right)a_2^--\left(-\frac{K}{EI}\,k_3-P_3k_3^2\right)a_3^-=0,\\
&\left(-\frac{K}{EI}\,k_1^2+P_1k_1^3\right)a_1^+\mathrm{e}^{-\mathrm{i}k_1L}+\left(-\frac{K}{EI}\,k_2^2+P_2k_2^3\right)a_2^+\mathrm{e}^{-\mathrm{i}k_2L}+\left(\frac{K}{EI}\,k_3^2+P_3k_3^3\right)a_3^+\mathrm{e}^{-k_3L}\\
&\quad+\left(-\frac{K}{EI}\,k_1^2+P_1k_1^3\right)a_1^-+\left(-\frac{K}{EI}\,k_2^2+P_2k_2^3\right)a_2^-+\left(\frac{K}{EI}\,k_3^2+P_3k_3^3\right)a_3^-=0,\qquad(32)\\
&\left(\frac{K}{GJ}\,\mathrm{i}P_1k_1^2-\mathrm{i}k_1\right)a_1^+\mathrm{e}^{-\mathrm{i}k_1L}+\left(\frac{K}{GJ}\,\mathrm{i}P_2k_2^2-\mathrm{i}k_2\right)a_2^+\mathrm{e}^{-\mathrm{i}k_2L}-\left(\frac{K}{GJ}\,P_3k_3^2+k_3\right)a_3^+\mathrm{e}^{-k_3L}\\
&\quad-\left(\frac{K}{GJ}\,\mathrm{i}P_1k_1^2-\mathrm{i}k_1\right)a_1^--\left(\frac{K}{GJ}\,\mathrm{i}P_2k_2^2-\mathrm{i}k_2\right)a_2^-+\left(\frac{K}{GJ}\,P_3k_3^2+k_3\right)a_3^-=0.
\end{aligned}$$

Eqs. (31) and (32) can be written in matrix form as

$$\mathbf{Aa}=\mathbf{0},\qquad(33)$$

where vector $\mathbf{a}=[a_1^+\ \ a_2^+\ \ a_3^+\ \ a_1^-\ \ a_2^-\ \ a_3^-]^{\mathrm{T}}$, and $\mathbf{A}$ is a 6 by 6 matrix in the form:

$$\mathbf{A}=\begin{bmatrix}
\alpha_{11} & \alpha_{12} & \alpha_{13} & \alpha_{14} & \alpha_{15} & \alpha_{16}\\
\alpha_{21} & \alpha_{22} & \alpha_{23} & \alpha_{24} & \alpha_{25} & \alpha_{26}\\
\alpha_{31} & \alpha_{32} & \alpha_{33} & \alpha_{34} & \alpha_{35} & \alpha_{36}\\
\alpha_{41} & \alpha_{42} & \alpha_{43} & \alpha_{44} & \alpha_{45} & \alpha_{46}\\
\alpha_{51} & \alpha_{52} & \alpha_{53} & \alpha_{54} & \alpha_{55} & \alpha_{56}\\
\alpha_{61} & \alpha_{62} & \alpha_{63} & \alpha_{64} & \alpha_{65} & \alpha_{66}
\end{bmatrix}.\qquad(34)$$

The coefficients α_{ij} $(i,j=1,\ldots,6)$ are not difficult to find from Eqs. (31) and (32).

Table 2
Natural frequencies of beam 1

Mode number	Natural frequency (Hz)							
	Ref. [2]	Ref. [6]	Ref. [7]	Section 4.1.1	Section 4.1.1 (approx.)	Section 4.1.2 (exact)	Section 4.1.2 (approx.)	Uncoupled (exact)*
1	4.3	4.66	4.66	4.7	4.7	4.7	4.7	4.8(b)
2	28	29.6	29.17	29.3	29.3	29.3	29.3	30.1(b)
3	78	84.89	81.63	81.8	81.8	81.8	81.8	84.1(b)
4	135	113.43	113.28	113.4	113.4	113.4	113.4	113.4(t)

*(exact), Wavenumbers solved from Eq. (9); (approx.), Wavenumbers approximated using k_t, k_{b1} and k_{b2}.

Table 3
Natural frequencies of beam 2

Mode number	Natural frequency (rad/s)						
	Ref. [2]	Ref. [4,7]	Section 4.1.1 (approx.)	Section 4.1.1 (exact)	Section 4.1.2 (approx.)	Section 4.1.2 (exact)	Uncoupled
1	8.040	8.040	8.2	8.2	8.2	8.2	8.8[(b)]
2	50.32	50.39	50.9	50.9	50.9	50.9	54.7[(b)]
3	141.4	141.0	141.4	141.4	141.4	141.4	152.7[(b)]
4	279.0	276.0	276.5	276.5	276.5	276.5	299.1[(b)]
5	306.0	304.3	304.7	304.7	304.7	304.7	304.1[(t)]
6			456.2	456.2	456.2	456.2	494.5[(b)]
7			680.5	680.5	680.5	680.5	738.3[(b)]
8			911.1	911.7	911.1	911.7	912.3[(t)]

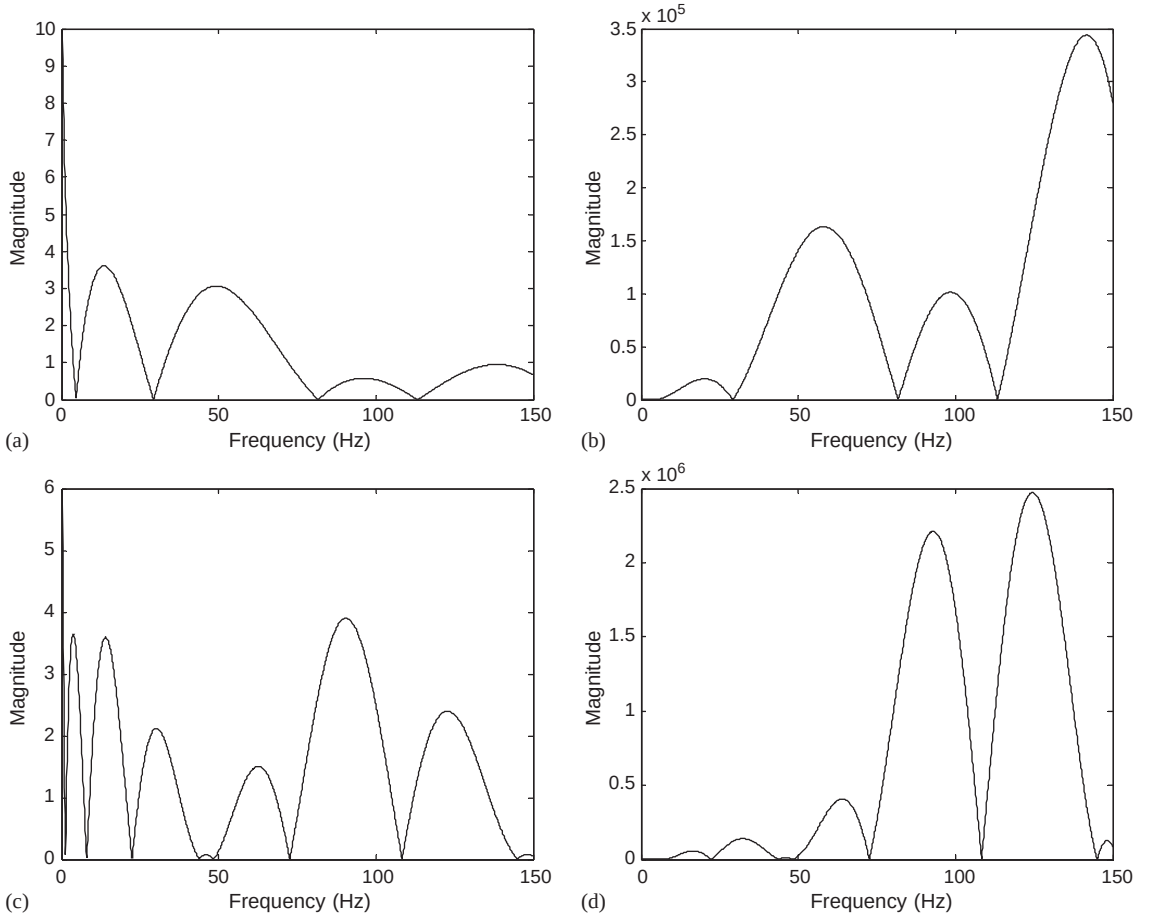

Fig. 7. Magnitude responses of the characteristic polynomials of (a) beam 1, obtained from Eq. (28), (b) beam 1, obtained from Eq. (35), (c) beam 2, obtained from Eq. (28), (d) beam 2, obtained from Eq. (35).

Setting the determinant of matrix **A** to zero, as is well known, gives the natural frequencies of the structure:

$$\mathbf{A} = \begin{vmatrix} \alpha_{11} & \alpha_{12} & \alpha_{13} & \alpha_{14} & \alpha_{15} & \alpha_{16} \\ \alpha_{21} & \alpha_{22} & \alpha_{23} & \alpha_{24} & \alpha_{25} & \alpha_{26} \\ \alpha_{31} & \alpha_{32} & \alpha_{33} & \alpha_{34} & \alpha_{35} & \alpha_{36} \\ \alpha_{41} & \alpha_{42} & \alpha_{43} & \alpha_{44} & \alpha_{45} & \alpha_{46} \\ \alpha_{51} & \alpha_{52} & \alpha_{53} & \alpha_{54} & \alpha_{55} & \alpha_{56} \\ \alpha_{61} & \alpha_{62} & \alpha_{63} & \alpha_{64} & \alpha_{65} & \alpha_{66} \end{vmatrix} = 0. \tag{35}$$

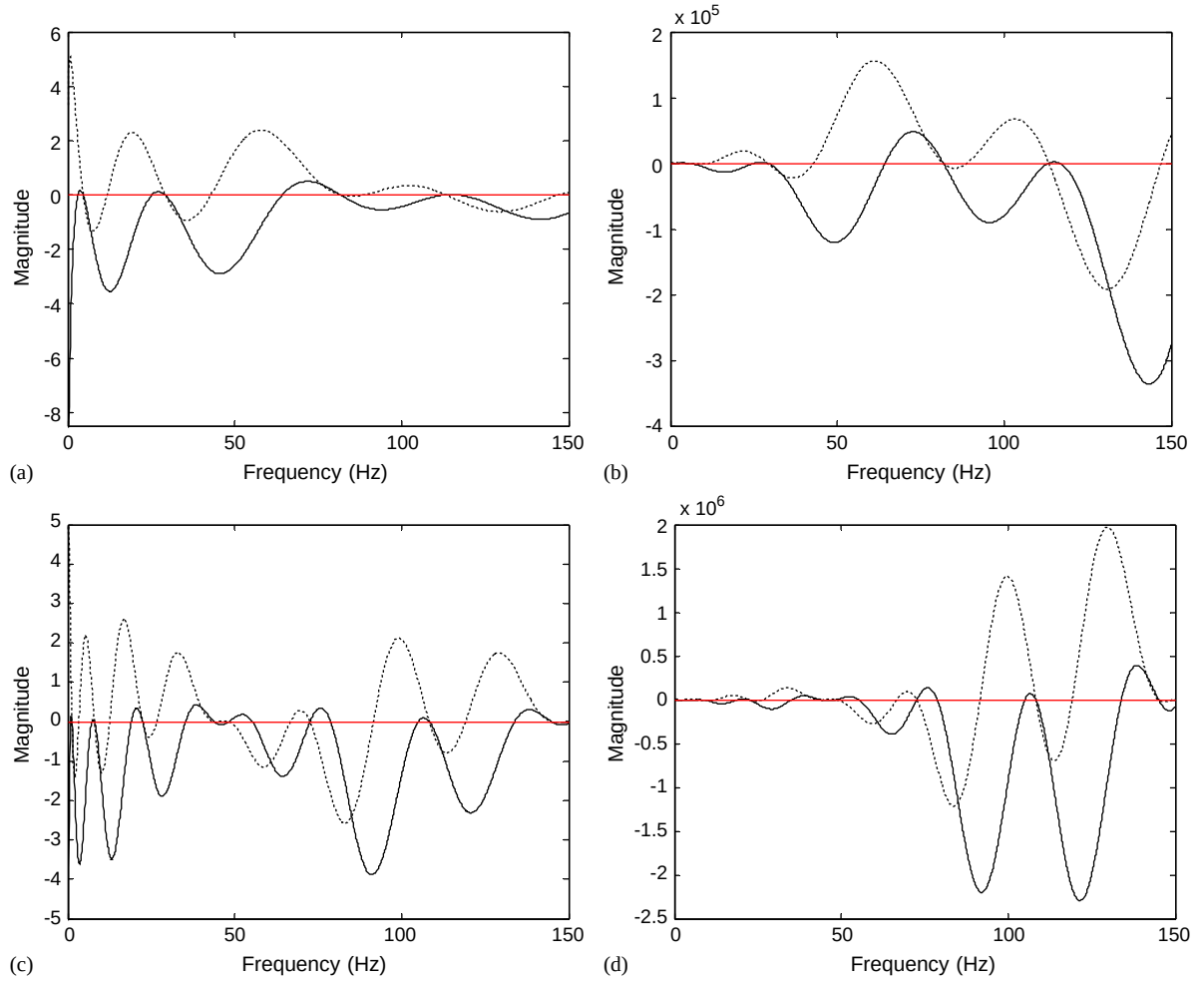

Fig. 8. Real (solid lines) and imaginary (broken lines) responses of the characteristic polynomials of (a) beam 1, obtained from Eq. (28), (b) beam 1, obtained from Eq. (35), (c) beam 2, obtained from Eq. (28), (d) beam 2, obtained from Eq. (35).

4.2. Mode shapes

Once the natural frequency is found, the mode shapes can be readily obtained by deleting one row of the 6 by 6 matrix and solving for the remaining five components of vector **a** in terms of the arbitrarily chosen component. An example arrangement is

$$\begin{bmatrix} \alpha_{11} & \alpha_{12} & \alpha_{13} & \alpha_{14} & \alpha_{15} \\ \alpha_{21} & \alpha_{22} & \alpha_{23} & \alpha_{24} & \alpha_{25} \\ \alpha_{31} & \alpha_{32} & \alpha_{33} & \alpha_{34} & \alpha_{35} \\ \alpha_{41} & \alpha_{42} & \alpha_{43} & \alpha_{44} & \alpha_{45} \\ \alpha_{51} & \alpha_{52} & \alpha_{53} & \alpha_{54} & \alpha_{55} \end{bmatrix} \begin{bmatrix} a_1^+ \\ a_2^+ \\ a_3^+ \\ a_1^- \\ a_2^- \end{bmatrix} = \begin{bmatrix} -\alpha_{16} \\ -\alpha_{26} \\ -\alpha_{36} \\ -\alpha_{46} \\ -\alpha_{56} \end{bmatrix} a_3^- . \tag{36}$$

Substituting $a_i^{\pm}$ $(i = 1, 2, 3)$ into Eqs. (29) and 30, one obtains the mode shapes of torsional rotation and transverse deflection of the centerline of the beam.

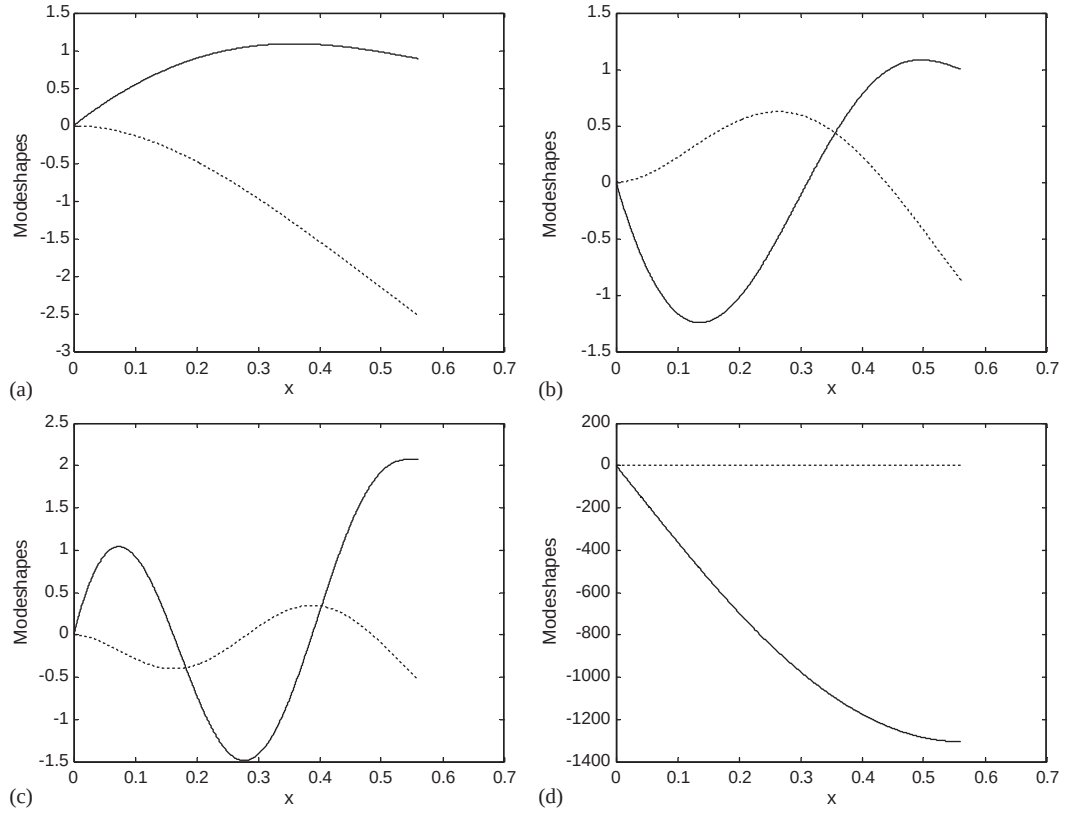

Fig. 9. Torsional rotation (solid lines) and flexural deflection (broken lines) mode shapes of beam 1: (a) first coupled mode, (b) second coupled mode, (c) third coupled mode, (d) pure torsional mode.

4.3. Numerical examples

The natural frequencies of the two example beams are listed in Tables 2 and 3. The natural frequencies of the uncoupled vibrations are listed in the last column with superscript b and t denoting bending and torsional vibrations, respectively. The coupled natural frequencies are obtained from Eqs. (28) and (35). Note that both equations are complex in nature. The natural frequencies are found either at those points with zero magnitudes or, equivalently, with both real and imaginary parts equaling zero. Fig. 7 shows the magnitude responses and Fig. 8 the real and imaginary responses obtained from Eqs. (28) and (35) of beams 1 and 2. The actual values of the natural frequencies are obtained through a self-written program in Matlab environment by recording simultaneous sign changes in both real and imaginary responses. The precision of the parameters can be as high as machine precision. Here the step size is chosen as 0.1 Hz, which is considered sufficient for comparison purposes.

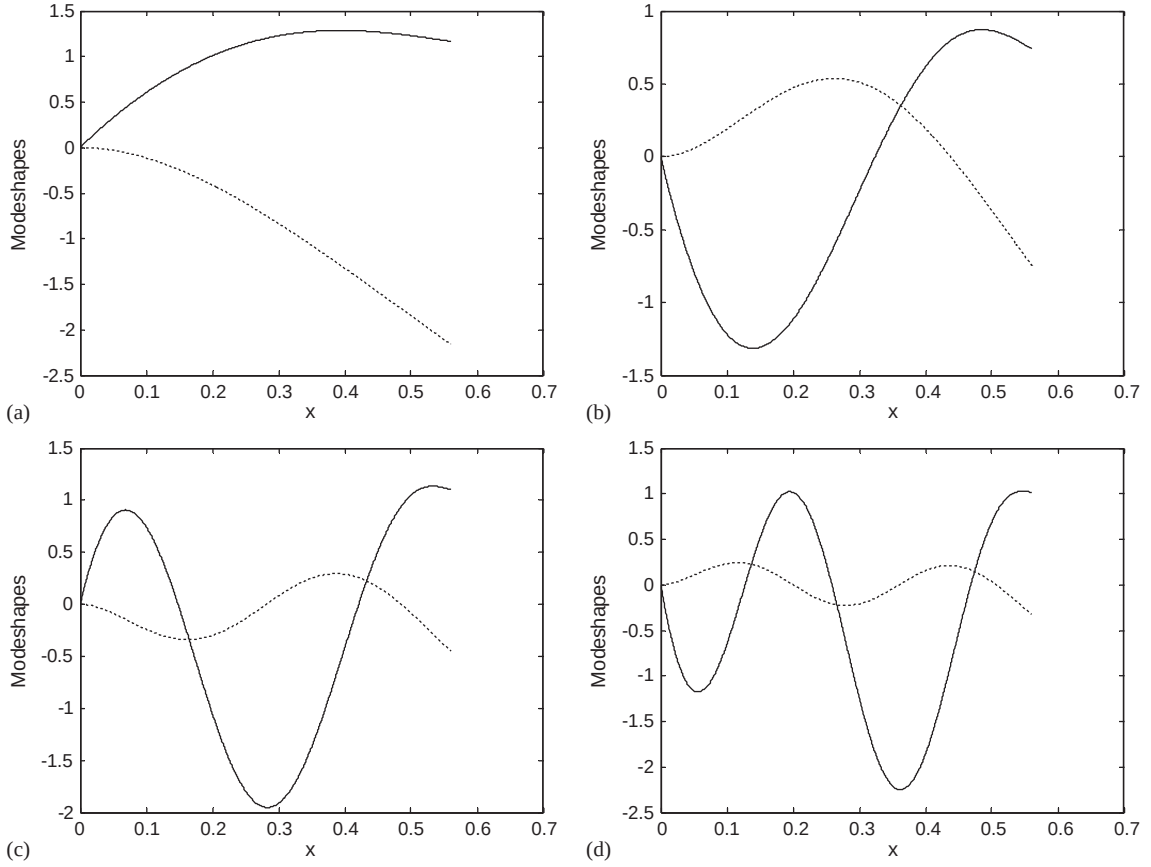

Fig. 10. Torsional rotation (solid lines) and flexural deflection (broken lines) mode shapes of beam 2: (a) first coupled mode, (b) second coupled mode, (c) third coupled mode, (d) fourth coupled mode, (e) pure torsional mode, (f) fifth coupled mode, (g) sixth coupled mode, (h) pure torsional mode.

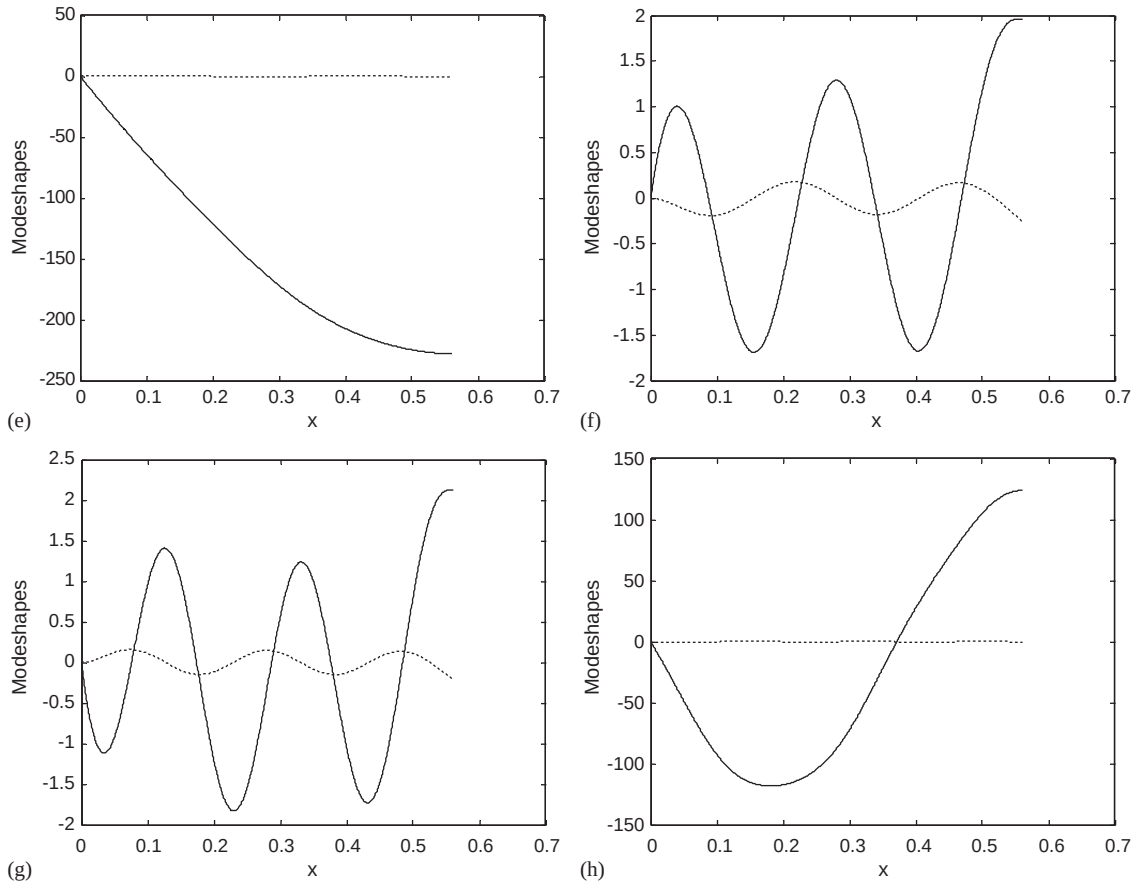

Fig. 10. (*Continued*)

It can be seen in Tables 1 and 2 that the natural frequencies calculated agree well with published results. The natural frequency values obtained in this study agree especially well among themselves. By comparing the coupled and uncoupled natural frequencies, it can be seen that bending vibration is more sensitive to material coupling than torsional vibration. Among bending modes, the higher frequency modes are far more sensitive to such a coupling effect.

Fig. 9 shows the mode shapes of the first four modes of beam 1. Fig. 10 shows the mode shapes of the first eight modes of beam 2. The fact that the pure torsional mode is less sensitive to the coupling effect than the bending mode at low frequencies is also reflected in the mode shape responses; see for example, the mode shapes plot (d) of beam 1 and plots (e) and (h) of beam 2. Which are essentially pure torsional modes themselves. However, apart from pure torsional modes, the rest of torsional modes due to coupling evolve to a shape resembling the mode shape in between the current and the next torsional mode in the case when there is no coupling.

5. Conclusions

The effect of coupling between bending and torsional deformations on vibrations of composite Euler–Bernoulli beams is studied from a wave standpoint. It is found that the dispersion characteristics, the natural frequencies and the mode shapes are in general affected by the material coupling except torsional mode at low frequencies. Higher frequency modes are more sensitive to such material coupling. Free vibration analysis is also performed from a wave standpoint, from which both natural frequencies and mode shapes are obtained. Numerical examples for which comparative results are available in the literature are presented and good agreement has been reached. The study offers guideline in choosing material, ply orientations and stacking sequence, which together determines the coupling coefficient, for favorable vibration characteristics. The results obtained in this paper are applicable to slender beams or structures that consist of slender beam components. For a deep beam, the shear deformation and rotary inertia must be taken into account.

References

[1] T.A. Weisshaar, B.L. Foist, Vibration tailoring of advanced composite lifting faces, *Journal of Aircraft* 22 (2) (1985) 141–147.
[2] P. Migunet, J. Dugundji, Experiments and analysis for composite blades under large deflection—Part I: static behavior—Part II: dynamic behavior, *AIAA Journal* 28 (1990) 1573–1588.
[3] R.B. Abarcar, P.F. Cunniff, The vibration of cantilever beams of fiber reinforced materials, *Journal of Composite Materials* 6 (1972) 504–517.
[4] J.R. Banerjee, Explicit analytical expressions for frequency equation and mode shapes of composite beams, *International Journal of Solids and Structures* 38 (2001) 2415–2426.
[5] D.H. Hodges, A mixed variational formulation based on exact intrinsic equations for dynamics of moving beams, *International Journal of Solids and Structures* 26 (1990) 1253–1273.
[6] D.H. Hodges, A.R. Atilgan, M.V. Fulton, L.W. Rehfield, Formulation and evaluation of an analytical model for composite box beams, *Journal of the American Helicopter Society* 36 (1991) 23–35.
[7] J.R. Banerjee, F.W. Williams, Free vibration of composite beams—an exact method using symbolic computation, *Journal of Aircraft* 32 (3) (1995) 636–642.
[8] D.J. Mead, Waves and modes in finite beams: application of the phase closure principle, *Journal of Sound and Vibration* 171 (5) (1994) 695–702.
[9] T.A. Weisshaar, R.J. Ryan, Control of aeroelastic instabilities through stiffness cross coupling, *Journal of Aircraft* 23 (2) (1986) 148–155.
[10] Members of the Mathematical Handbook Editorial Group, *Mathematical Handbook*, Higher Education Publications, Beijing, 1977 (in Chinese).
[11] D.J. Inman, *Engineering Vibration*, Prentice-Hall International, Englewood Cliffs, NJ, 1994.